

Direct Measurement of Dissipation in the $^{35}\text{Cl} + ^{12}\text{C}$ Reaction at 43 MeV/nucleon

L. Beaulieu,¹ Y. Larochelle,¹ L. Gingras,¹ G. C. Ball,² D. R. Bowman,² B. Djerroud,^{1,*} D. Doré,^{1,†}
 A. Galindo-Uribarri,² D. Guinet,³ E. Hagberg,² D. Horn,² R. Laforest,^{1,‡} P. Lautesse,³ R. Roy,¹
 M. Samri,¹ and C. St-Pierre¹

¹Laboratoire de Physique Nucléaire, Département de Physique, Université Laval, Québec, Canada G1K 7P4

²Atomic Energy of Canada Limited, Chalk River Laboratories, Ontario, Canada K0J 1J0

³Institut de Physique Nucléaire de Lyon, 46 Bd du 11 Novembre 1918, F-69622 Villeurbanne Cedex, France

(Received 19 January 1996)

Characteristics of $^{35}\text{Cl} + ^{12}\text{C}$ collisions at 43 MeV/nucleon have been studied for events with total charge detected ($\Sigma Z = 23$). It is shown that, while single-source events are present in the data, the binary nature of the collision is dominant. For binary events, the emitting sources (projectilelike and targetlike) were reconstructed independently allowing a direct measurement of the total dissipated energy. It is found that up to 75% of the available energy is dissipated and the significant momentum transfer of the selected events leads to the "equal temperature limit." [S0031-9007(96)00514-5]

PACS numbers: 25.70.Lm, 25.70.Mn

Heavy ion collisions in the intermediate energy range, from 10 to 100 MeV/nucleon, produce highly excited nuclei. One of the dominant exit channels observed in these reactions is nuclear multifragmentation [1], where the system breaks into many fragments ($Z \geq 3$). The deexcitation mechanism competes with well-known low energy processes such as fusion/fission or deep inelastic reactions [2], as well as nucleon-nucleon scattering, typical of high energy. Despite numerous experimental results, a satisfactory explanation for multifragmentation, either statistical or dynamical, is still lacking [1]. Recently, a new challenge has arisen in understanding the dissipation stage of such reactions, i.e., the persistence of the binary character of the collision even in very violent or "central" collisions [3–7]. Using neutrons and light charged particles (LCP) as independent measurements of excitation or dissipated energy, Lott *et al.* [3] have shown that binary mechanisms dominate the cross section for any degree of dissipation, including that usually associated with central collisions. In the $^{208}\text{Pb} + ^{197}\text{Au}$ system studied by Lecolley *et al.* [4], a similar analysis was made for central events selected from LCP multiplicities. For total-kinetic-energy losses up to complete damping, the evolution of the binary reaction mechanism appeared independent of intermediate-mass fragment multiplicity. These measurements on heavy systems at beam energies just below the Fermi energy were in agreement with dissipative orbiting [4,8]; however, single-source events (compound nuclei) were not eliminated from the analysis.

In this Letter we present the first analysis in which a careful selection of the binary events is made and the degree of dissipation is evaluated by complete kinematic reconstruction of the projectilelike emitter (PLE) and targetlike emitter (TLE) from their respective charged decay products.

The experiment was performed at the Tandem Accelerator Superconducting Cyclotron (TASCC) at Chalk River. A beam of ^{35}Cl at 43 MeV/nucleon bombarded a 2.2

mg/cm² thick carbon target. The reaction products were detected in an array of 83 detectors covering polar angles from 3.0° to 46.8°. The 80 detectors of the Laval-Chalk River forward array [9,10] are mounted in five concentric rings around the beam axis and cover nearly 100% of the solid angle between 6.8° and 46.8°. The first three rings are made of plastic phoswich detectors with a detection threshold of 7.5 (22.5) MeV/nucleon for $Z = 1$ (17) particles. The two outer rings are composed of CsI(Tl) crystals which achieve isotopic resolution for $Z = 1$ and 2 ions with a threshold of 2 MeV/nucleon and element identification for $Z = 3$ and 4 ions with a threshold of 5 MeV/nucleon. Three Si-CsI telescopes sample the most forward angles, 3.0° to 5.0°, and provide charge identification with a detection threshold of 2 (5) MeV/nucleon for $Z = 2$ (17) particles. The detection efficiency of the array for $Z = 1$ to 3 was evaluated from the angular distributions and was approximately constant at 75%; for higher Z it decreased smoothly to 5% for $Z = 12$. Only events where the total charge $\Sigma Z = 23$ was detected were retained for this analysis. A total of 2×10^5 complete events were recorded in both "minimum-bias" and central triggering conditions (charged-particle multiplicities ≥ 2 and ≥ 6 , respectively). In all steps of the analysis, the results are the same as those obtained from events where 1, 2, or 3 charge units are missing. However, those events were not included in the main sample because they would introduce ambiguities in the evaluation of the excitation energy.

The direct measurement of dissipation in the binary scenario is the ultimate goal of the present work. The events with a single emitter must first be rejected without removing the dissipative binary events. The centrality of an event has commonly been correlated to the charged particle (CP) multiplicity [11,12]. It is not used here because of the small range in CP multiplicities for a system as light as ours. Instead, two other observables were used as selection criteria of centrality: the total transverse energy [13] (similar to total transverse momentum [14]) and the

flow angle [4]. This last quantity is derived from event-shape analysis using the momentum tensor [15]:

$$T_{i,j} = \sum_{n=1}^{N_{CP}} P_i^{(n)} P_j^{(n)}; \quad i, j = 1, 2, 3, \quad (1)$$

where $P_i^{(n)}$, $P_j^{(n)}$ are the i th or j th Cartesian components of the particle momentum in the center of mass (c.m.) of the system and N_{CP} is the total number of charged particles in the event. The three eigenvalues and eigenvectors calculated from this tensor define the shape of the event. The angle between the major axis of the event in momentum space (the eigenvector with the largest eigenvalue) and the beam axis is Θ_{flow} , the flow angle.

Figure 1 shows the experimental yield of total transverse energy (E_{\perp}) versus Θ_{flow} for completely detected events. A weak correlation between the two observables can be seen from Θ_{flow} of 20° to about 60° , which might indicate that these observables do not select the same class of events. In order to evaluate the validity of both observables for selecting single source events, Fig. 2 displays perpendicular versus parallel velocity component in the c.m. for particles with $Z = 3$. In the left-hand panels of the figure, the parallel velocity is defined with respect to the beam axis, whereas for the right side it is defined with respect to the flow axis [Eq. (1)]. The effects of the energy thresholds and angular coverage of the detectors can be seen on the left, while the shapes of the emission patterns are evident on the right.

A first cut is made on Θ_{flow} (upper panels: $\Theta_{flow} < 30^{\circ}$) which includes 19% of the events. The binary nature is clearly seen in both frames with shapes characteristic of the PLE ($V_{\parallel} \sim 0.05c$) and TLE ($V_{\parallel} \sim -0.15c$) emission components. The strong backward emission of lithium in the

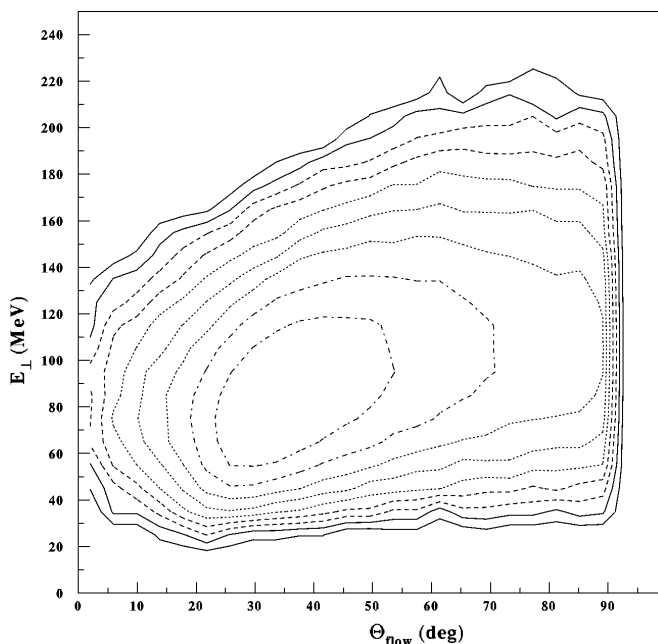


FIG. 1. Transverse energy vs flow angle for events with $\Sigma Z = 23$ in the $^{35}\text{Cl} + ^{12}\text{C}$ reaction at 43 MeV/nucleon. 2×10^5 experimental events are shown; each contour represents a factor of 2.

center of mass is compensated mainly by forward emission of heavier fragments ($Z > 6$), while the reverse situation with the heavier fragments emitted backwards would not pass the detector thresholds. Particles with $Z = 2$ or $Z = 4$ have similar characteristics to those of $Z = 3$. The selected events ($\Theta_{flow} < 30^{\circ}$) do not include the most peripheral collisions, since the grazing angle is about 1° for this reaction, and our detector coverage starts at 3° . The array is also partly insensitive to incomplete fusion, since targetlike preequilibrium backward proton emission would rarely be detected [16]. This plot also shows the presence of particles with velocities around $V_{\parallel} \sim -0.07c$. They may originate from a single source or be intermediate residues (necklike structures). Such a contribution has been evaluated to be at most 10% of the cross section [17]. Therefore binary dissipative events are dominant and account for at least 90% of the cross section at low Θ_{flow} .

If, instead, large values of Θ_{flow} are selected (middle panels: $\Theta_{flow} > 75^{\circ}$), the emission pattern is typical of a single source, with a residual ellipsoid shape along the major axis because of its finite multiplicity. Those events correspond to full damping of the kinetic energy.

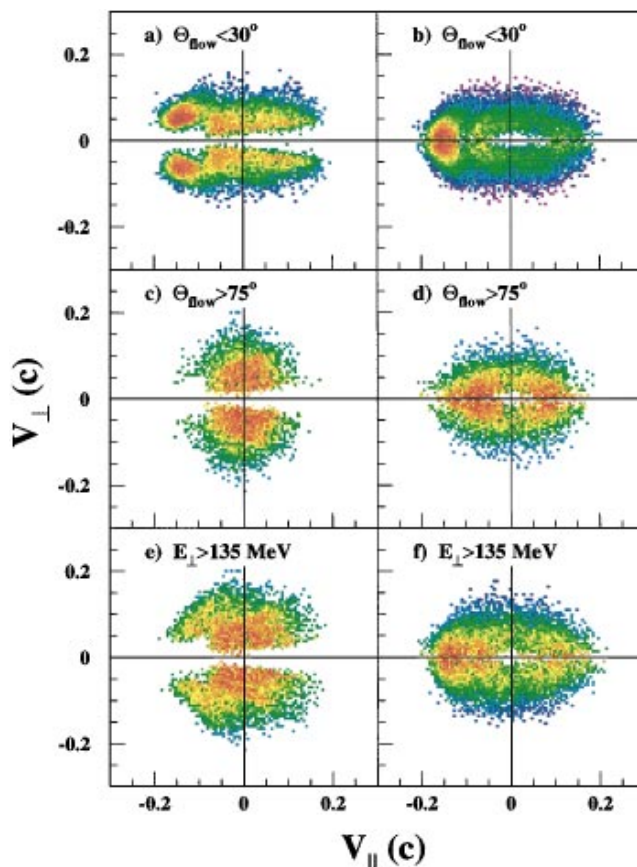


FIG. 2 (color). Galilean invariant perpendicular vs parallel velocity in the c.m. frame for $Z = 3$ fragments. Parallel velocities are along the beam axis [(a),(c),(e)] and the main axis of the momentum tensor [(b),(d),(f)]. Cuts on $\Theta_{flow} < 30^{\circ}$ [(a),(b)], $\Theta_{flow} > 75^{\circ}$ [(c),(d)], and on $E_{\perp} > 135$ MeV (top 10% of the distribution: [(e),(f)]) are made. The count yield is in a logarithmic scale.

They account for 10% of the detected events, or 4% of the efficiency-corrected reaction cross section; the total geometric cross section of the reaction is estimated at 2 b. A smaller fraction of the total reaction cross section, 1%, was recently found by Péter *et al.* for the $^{36}\text{Ar} + ^{27}\text{Al}$ system [7]. Single-source events have also been seen in the $^{35}\text{Cl} + ^{12}\text{C}$ reaction at 35 MeV/nucleon [18].

The bottom panels of Fig. 2 show $Z = 3$ velocity distributions for events having $E_{\perp} > 135$ MeV, corresponding to the 10% of the events with the highest transverse energy. This selection, commonly used to isolate central events, is less successful in selecting the single-source events. Targetlike remnants can still be seen, although less strongly than in the top panels. This observation indicates either that a 10% cut in E_{\perp} is not selective enough for single-source events or that transverse energy is not the best observable to distinguish between single- and binary-source events. For the present analysis, the optimum selection of binary-source events is achieved with $\Theta_{\text{flow}} < 65^{\circ}$. Completely damped binary events might still be present at higher flow angle values but they are indistinguishable from single-source events.

After the binary-source events had been isolated, the emitters were reconstructed by the following procedure:

(1) After selecting only completely detected events and removing $Z = 1$ particles, we used a variant of the thrust method [15] to correlate each CP to an emitter. The thrust is defined as [19]

$$\text{Thrust} = \text{maximum} \left(\frac{|\sum_i \vec{p}_i| + |\sum_j \vec{p}_j|}{\sum_{k=1}^{N_{\text{CP}}} |\vec{p}_k|} \right), \quad (2)$$

where \vec{p}_i and \vec{p}_j are the momentum vectors of the particles in the c.m. for all possible i, j combinations of the N_{CP} particles in any two groups and \vec{p}_k the momentum vector for all particles. The thrust is the combination giving the maximum possible separation in momentum space between two groups of particles which are then assigned to the PLE and the TLE. The PLE velocity \vec{V}_{PLE} and the TLE velocity \vec{V}_{TLE} , relative to the c.m., could then be reconstructed.

(2) The $Z = 1$ particles are assigned to the PLE or to the TLE by a projection on the $\vec{V}_{\text{PLE}} - \vec{V}_{\text{TLE}}$ axis of their velocity vector in the c.m., with the separation point obtained from the mass ratio of the two emitters.

(3) The emitter velocities are then reevaluated with the $Z = 1$ particles included. As the projectile is a chlorine nucleus ($Z = 17$), only events with $Z_{\text{PLE}} = 15, 16, 17$, or 18 were kept; this criterion selects events with minimal net transfer and good intersource separation, reinforcing the flow angle cut. The remaining events account for 48% of the total statistics. A test with filtered binary-source EUGENE [20] simulations showed that under the present conditions more than 75% of particles with $Z = 1$ to 3 were assigned to the proper emitter; this percentage increases to 100% for $Z > 5$.

(4) Finally, the excitation energy is deduced for each emitter from the total relative kinetic energy and from

the Q value of each channel, including a correction for the undetected neutrons [21]. The sum of the excitation energy and kinematic energies of both emitters averages 338 ± 58 MeV, i.e., 88% of the total available energy.

The reconstruction procedure was validated by comparing the experimental dissipated energy to the value of filtered simulations. This comparison must be done with the same global event shape which was verified using the anisotropy ratio [22] as a measure of event shape. The anisotropy distribution for experimental events with $\Sigma Z = 23$, $\Theta_{\text{flow}} < 65^{\circ}$, and $15 \leq Z_{\text{PLE}} \leq 18$ was centered at $R_A = 0.65$, and was well reproduced with binary-source EUGENE simulations with an impact parameter ranging from 4 to 6 fm. The effect of preequilibrium emission on R_A was explored with the code GENEVE [23] and was found to be unimportant. More details can be found in Ref. [16].

The top panels in Fig. 3 show the excitation energy ratio between the PLE and the TLE as a function of Θ_{flow} and E_{\perp} . Also plotted are the filtered and unfiltered EUGENE simulations. The filtering process including the effect of the reconstruction procedure increases the energy ratio ($E_{\text{proj}}^*/E_{\text{target}}^*$) by about 20%. The experimental ratio is close to the ratio of the projectile mass to the target mass, a feature typical of the equal temperature limit [24], in that equal amounts of energy per nucleon appear to be dissipated in the projectile and target. The bottom panels show the total dissipated energy and present a puzzling picture. The dissipated energy varies little with Θ_{flow} and its average corresponds to 65% of the c.m. energy. The

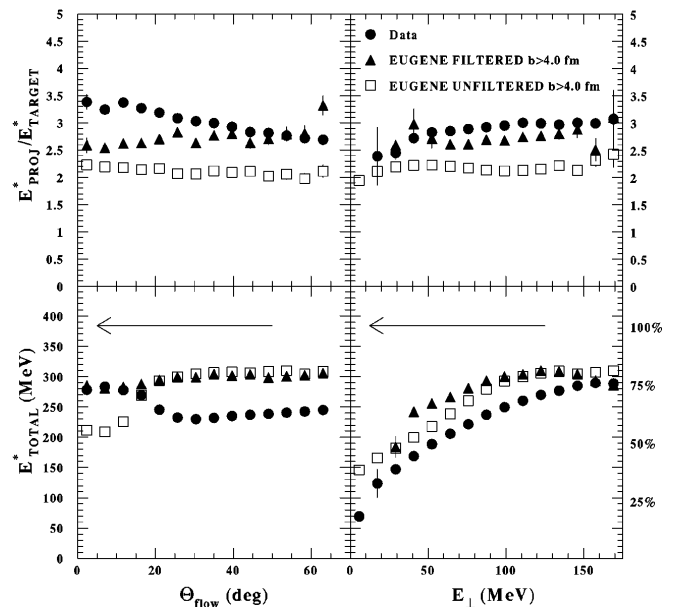


FIG. 3. Ratio of excitation energy for PLE and TLE (top panels) and total excitation energy vs the flow angle (left panels) and total transverse energy (right panels). The data (full dots), the filtered (full triangles), and the unfiltered (open squares) EUGENE simulations are plotted. Symbols represent the average for each bin and error bars, shown when larger than the symbol, are the standard error of the mean. Arrows indicate the c.m. energy (100% damping).

unfiltered simulation seems to indicate a small correlation between the two observables at Θ_{flow} below 20° , but this correlation is completely washed out by the effects of the experimental filter since very peripheral collisions remain undetected.

In contrast, the right panel of Fig. 3 exhibits a significant increase in dissipation, from 20% to 75% of the total c.m. energy, with increasing transverse energy. Again the experimental results are well reproduced by the filtered EUGENE simulations. On the one hand, the trend observed as a function of E_\perp is as expected for an observable correlated to the impact parameter: As the impact parameter decreases, the transverse energy increases. On the other hand, Fig. 1 shows that the largest flow angles ($\Theta_{\text{flow}} > 75^\circ$) have a broad range of transverse energies and Fig. 3 shows dissipation to be independent of flow angle, which is geometrically linked to impact parameter. Therefore, for the relatively light system and large momentum transfers studied here, dissipation is not necessarily correlated with “centrality” (in the sense of geometric trajectories with small impact parameter).

In summary, it has been shown that a selection based on flow angle was successful in separating the dominant binary-source events from single-source events. A momentum-based method can be used to reconstruct independently both the PLE and the TLE and to deduce their excitation energy in dissipative binary collisions between “light” heavy ions. The total excitation energy is correlated with the transverse energy and the degree of dissipation has been observed up to 75% of the available energy. The excitation-energy sharing follows the equal-temperature limit over a complete range of flow angle and transverse energy for the high-momentum-transfer events selected by the total charge requirement. We have shown that the relation between dissipation, geometric centrality, and the number of emitters in the exit channels for light systems differs from the standard picture in which central reactions are much more violent and dissipative than midcentral ones. Another possibility is that central collisions of light heavy ions in the Fermi energy range produce mainly binary events. Dynamical models [25] may shed new light on this challenging problem.

We would like to thank Dr. D. Durand and Dr. J.-P. Wieleczko for the use of their statistical codes. This work was supported in part by the Natural Sciences and

Engineering Research Council of Canada and the Fonds pour la Formation de Chercheurs et l’Aide à la Recherche.

-
- *Present address: NSRL, University of Rochester, 271 East River Road, Rochester, NY 14627.
 †Present address: Institut de Physique Nucléaire d’Orsay, B.P. 91406, Orsay Cedex, France.
 ‡Present address: AECL Research, Chalk River Laboratories, Ontario, Canada K0J 1J0.
- [1] L. G. Moretto and G. J. Wozniak, *Annu. Rev. Nucl. Part. Sci.* **43**, 379 (1993), and references therein.
 [2] W. U. Schröder and J. R. Huizenga, in *Treatise on Heavy-Ion Science*, edited by D. A. Bromley (Plenum, New York, 1984), Vol. 2, p. 115.
 [3] B. Lott *et al.*, *Phys. Rev. Lett.* **68**, 3141 (1992).
 [4] J. F. Locolley *et al.*, *Phys. Lett. B* **325**, 317 (1994).
 [5] B. M. Quednau *et al.*, *Phys. Lett. B* **309**, 10 (1993).
 [6] Y. Larochelle *et al.*, *Phys. Lett. B* **352**, 8 (1995).
 [7] J. Péter *et al.*, *Nucl. Phys.* **A593**, 95 (1995).
 [8] S. P. Baldwin *et al.*, *Phys. Rev. Lett.* **74**, 1299 (1995).
 [9] C. Pruneau *et al.*, *Nucl. Instrum. Methods Phys. Res., Sect. A* **297**, 404 (1990).
 [10] Y. Larochelle *et al.*, *Nucl. Instrum. Methods Phys. Res., Sect. A* **348**, 167 (1994).
 [11] D. R. Bowman *et al.*, *Phys. Rev. C* **46**, 1834 (1992).
 [12] M. B. Tsang *et al.*, *Phys. Rev. Lett.* **71**, 1502 (1993).
 [13] M. A. Lisa *et al.*, *Phys. Rev. Lett.* **70**, 3709 (1993).
 [14] G. D. Westfall *et al.*, *Phys. Rev. Lett.* **71**, 1986 (1993).
 [15] J. Cugnon *et al.*, *Nucl. Phys.* **A397**, 519 (1983).
 [16] Y. Larochelle *et al.*, *Phys. Rev. C* **53**, 823 (1996).
 [17] Y. Larochelle *et al.* (to be published).
 [18] D. Horn *et al.*, in *Proceedings of the Workshop on Heavy-Ion Fusion, Padua, Italy, 1994*, edited by A. M. Stefanini, G. Nebbia, S. Lunardi, G. Montagnoli, and V. Vitturi (World Scientific, Singapore, 1995).
 [19] V. Métivier, Ph.D. thesis, Université de Caen, 1995 (unpublished).
 [20] D. Durand, *Nucl. Phys.* **A541**, 266 (1992).
 [21] J. C. Steckmeyer *et al.*, *Nucl. Phys.* **A500**, 372 (1989).
 [22] H. Ströbele *et al.*, *Phys. Rev. C* **27**, 1349 (1983).
 [23] J. P. Wieleczko, E. Plagnol, and P. Ecomard, in *Proceedings of the 2nd TAPS Workshop, 1994*, edited by Martinez Diaz and Guardemar Schutz (World Scientific, Singapore, 1995), p. 145.
 [24] J. Töke and W. U. Schröder, *Annu. Rev. Nucl. Part. Sci.* **42**, 401 (1992), and references therein.
 [25] G. Peilert *et al.*, *Rep. Prog. Phys.* **57**, 533 (1994).